The Warm/Hot Universe

Summary

Neta A. Bahcall
Princeton University

The Hot Universe: Clusters

- Powerful tool for Cosmology
- Powerful tool for Tracing Large Scale Structure
- Growth of structure
- ICM physics; heating, cooling, non-thermal, soft & hard excess, AGN, metalicities; Evolution of the ICM

The Warm Universe: IGM

- Where are the other baryons?
- Tracing the IGM and Large-scale Structure
- Cosmology; comparison with simulations

Test MOND

Clusters: Powerful Tool for Cosmology

- Cluster Mass (Temp) Function and its Evolution
  - → σ_8 Ω_m Ω_Λ ω (need accurate M_{cl})
- Baryon (Gas) Fraction and its Evolution
  - → Ω_m Ω_Λ ω (understand ICM evolution)
- Baryon Acoustic Oscillations using Clusters
  - → Ω_m Ω_Λ ω ('Standard Ruler')
- Cluster Shape → σ_8 Ω_m ω
- M/L Function → Ω_m

Cluster Abundance and Evolution

- *Powerful method to determine* Ω_m, σ_8, w

  σ_8 = *Amplitude of mass fluctuations*
- n_{cl} (z~0) → $\sigma_8 \Omega_m^{0.6} \sim 0.35$ (MF Shape → σ_8)
- n_{cl} (hi z) → *Breaks degeneracy*

→ Ω_m=0.2+-0.05 and σ_8=0.9+-0.1

- *Need accurate Mass calibration for precision cosmology*

◆◆◆◆◆◆◆◆◆◆◆◆◆◆◆◆◆◆◆◆◆◆◆◆◆◆◆◆◆◆◆◆◆◆◆

- σ_8 (galaxies)(obs) ~ 0.9
- *If* **Mass ~ Light** *(on large scale)* → σ_8(m)~ 0.9

Mass-Function SDSS Clusters

(Bahcall, Dong, et al '02)

Best-fit MF: Ω_m=0.2 and σ_8=0.9

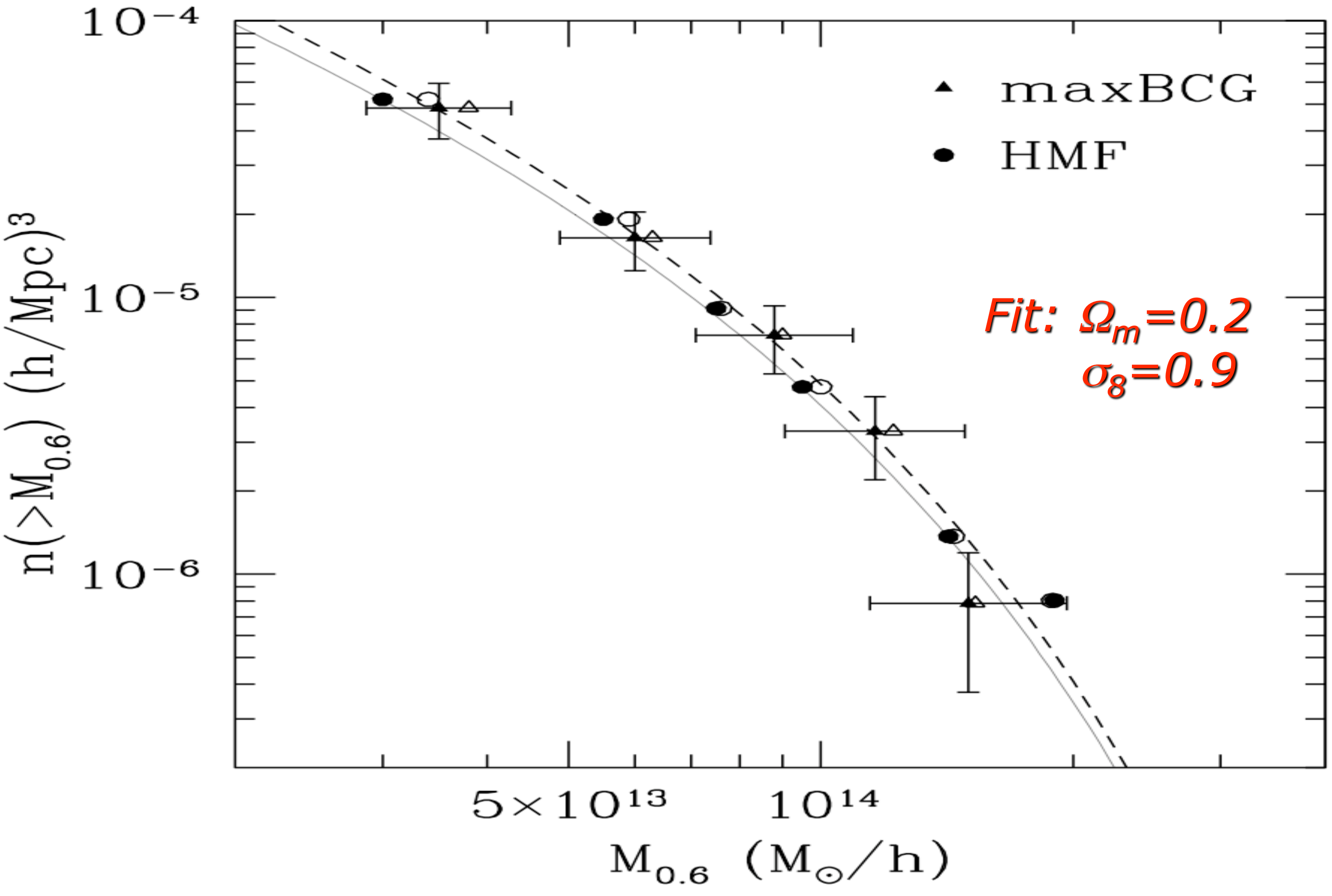

Ω_m - σ_8 (Clusters MF) (Bahcall, Dong etal '03)

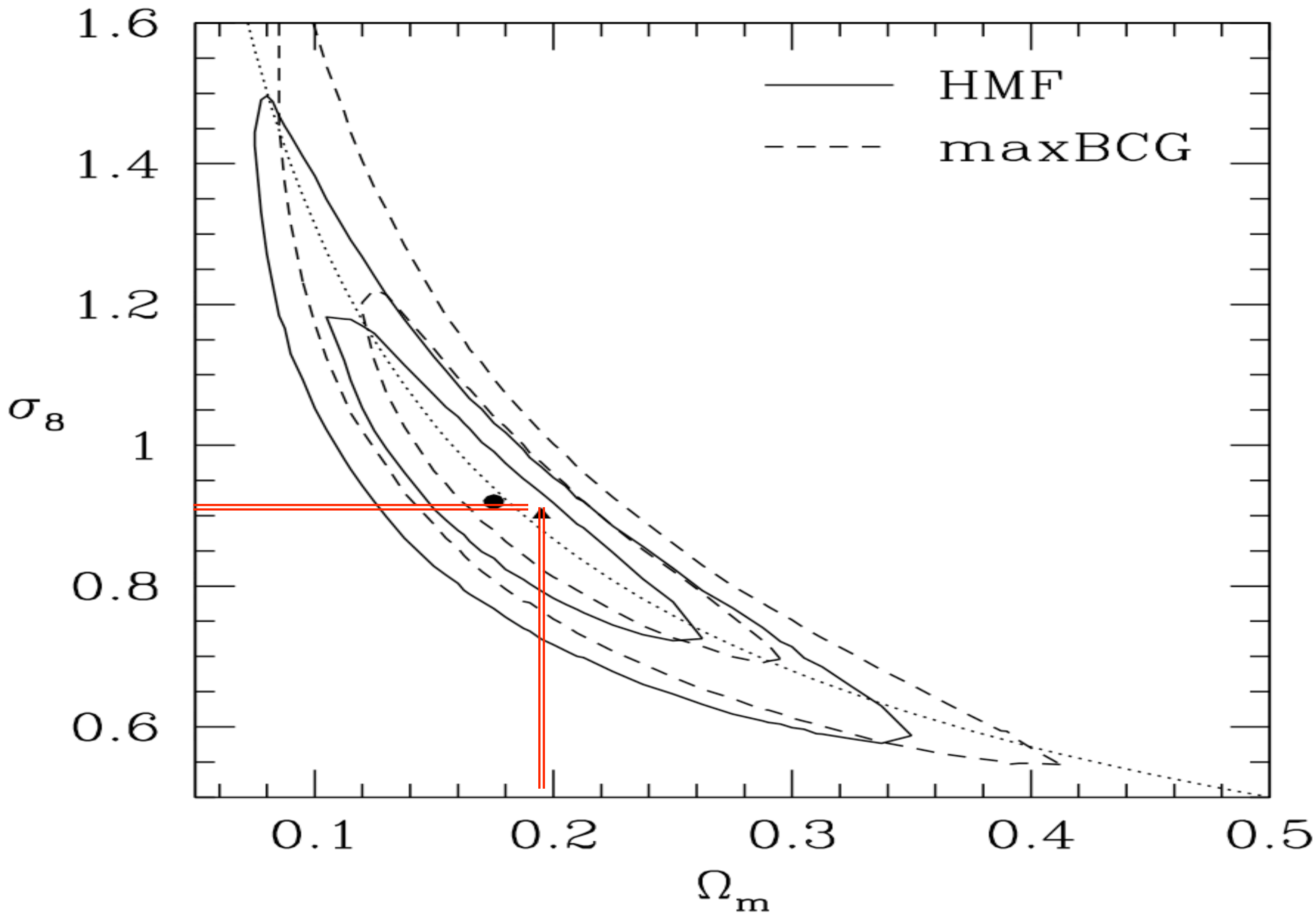

Cluster Abundance Evolution → σ_8

(Bahcall & Bode '03)

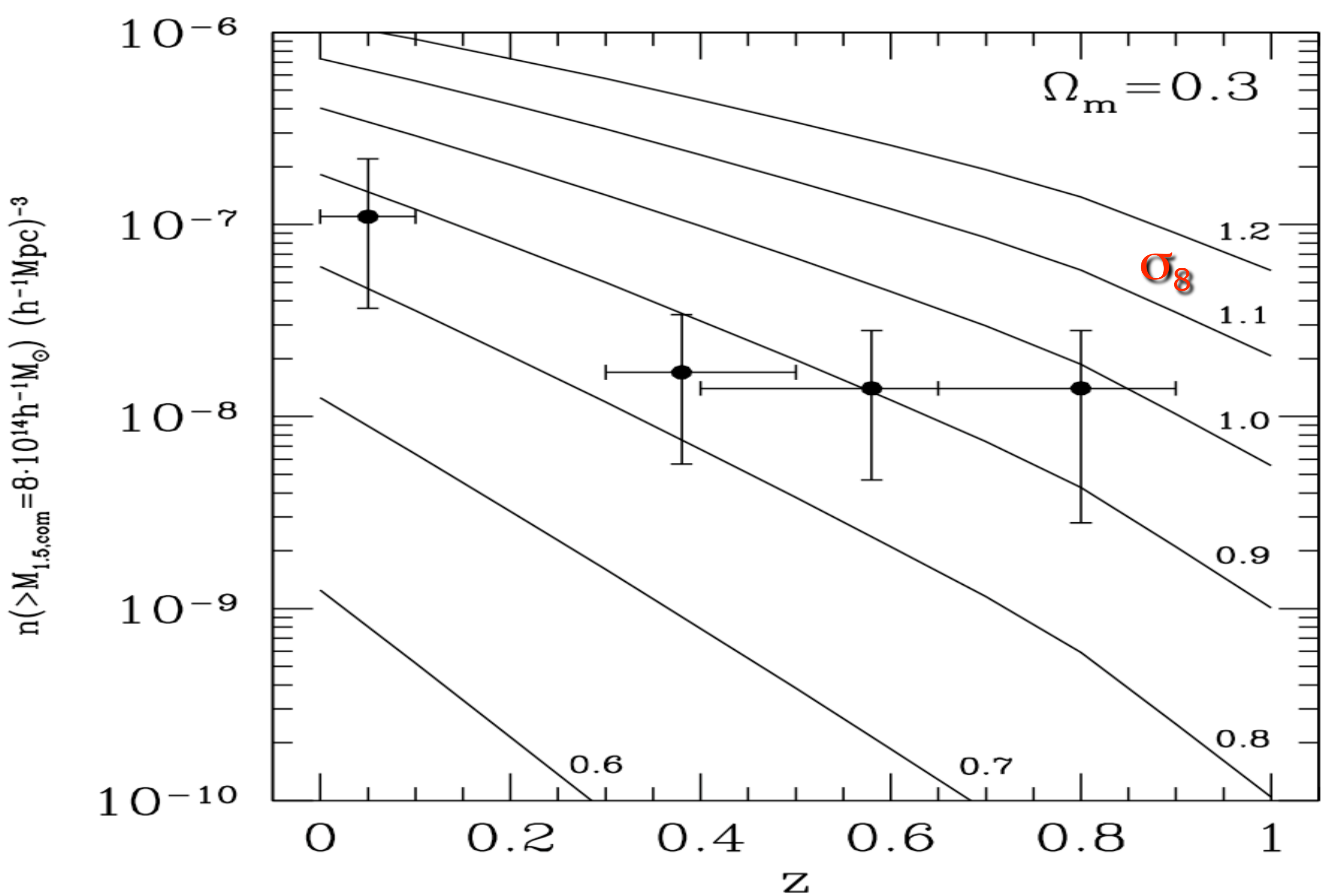

Cosmological Constraints (Bahcall & Bode)
(from Low and Hi redshift cluster abundance)

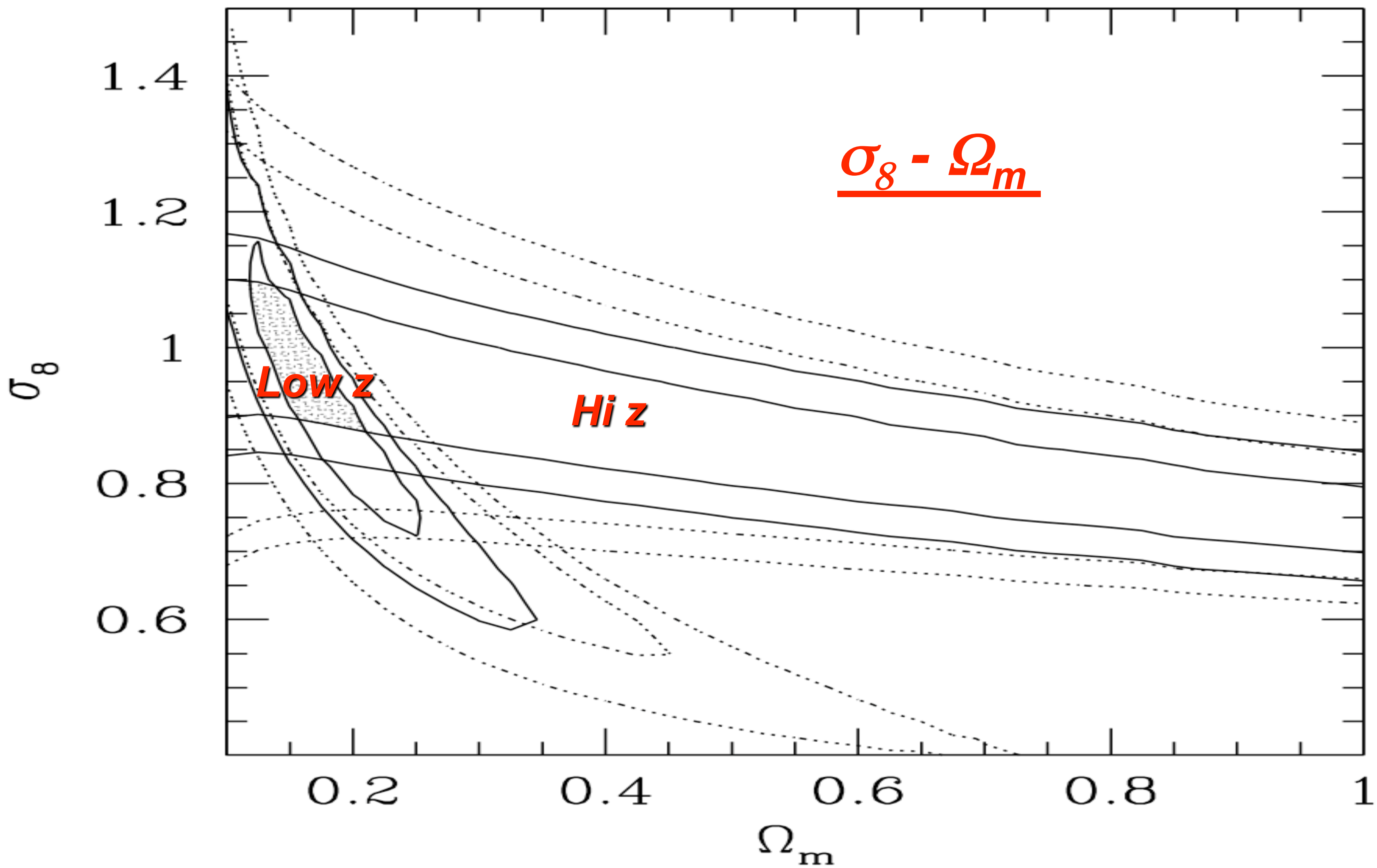

Evolution of Cluster XLF (Mantz etal 08)

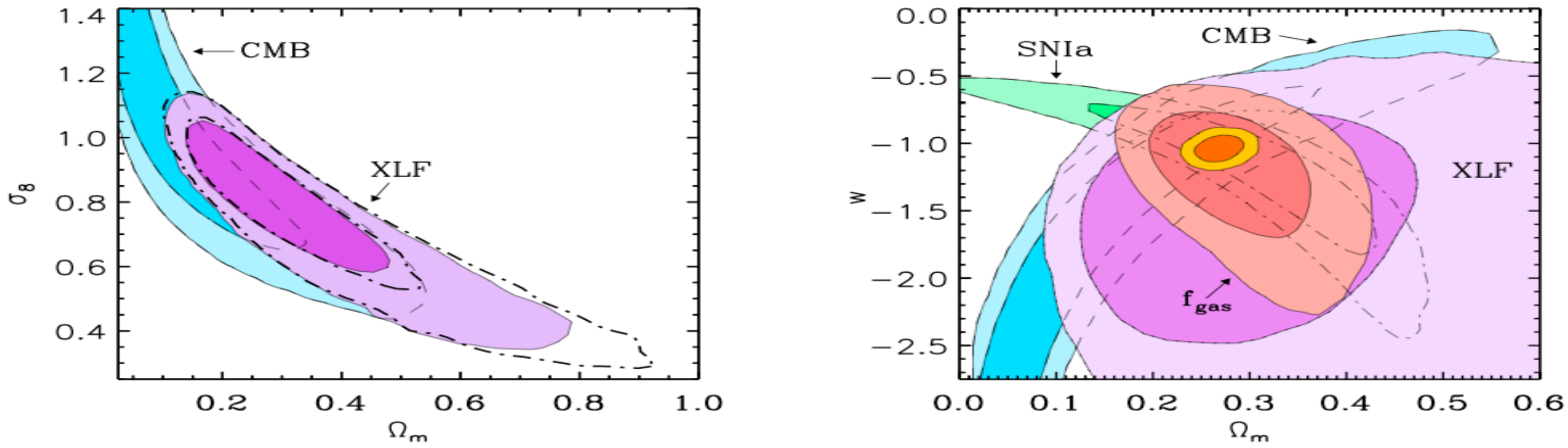

Figure 9. Joint 68.3 and 95.4 per cent confidence constraints on Ω_m and σ_8 (left) and Ω_m and w (right) for a constant-w model using the X-ray luminosity function data (purple) and standard priors (Table 1). Also shown are independent constraints from the CMB (blue; Spergel et al. 2007), SNIa data (green; Davis et al. 2007) and cluster f_{gas} data (red Allen et al. 2008), and the combination of all four (gold). In the left panel, the dot-dashed lines indicate the XLF results using our weak prior on n_s.

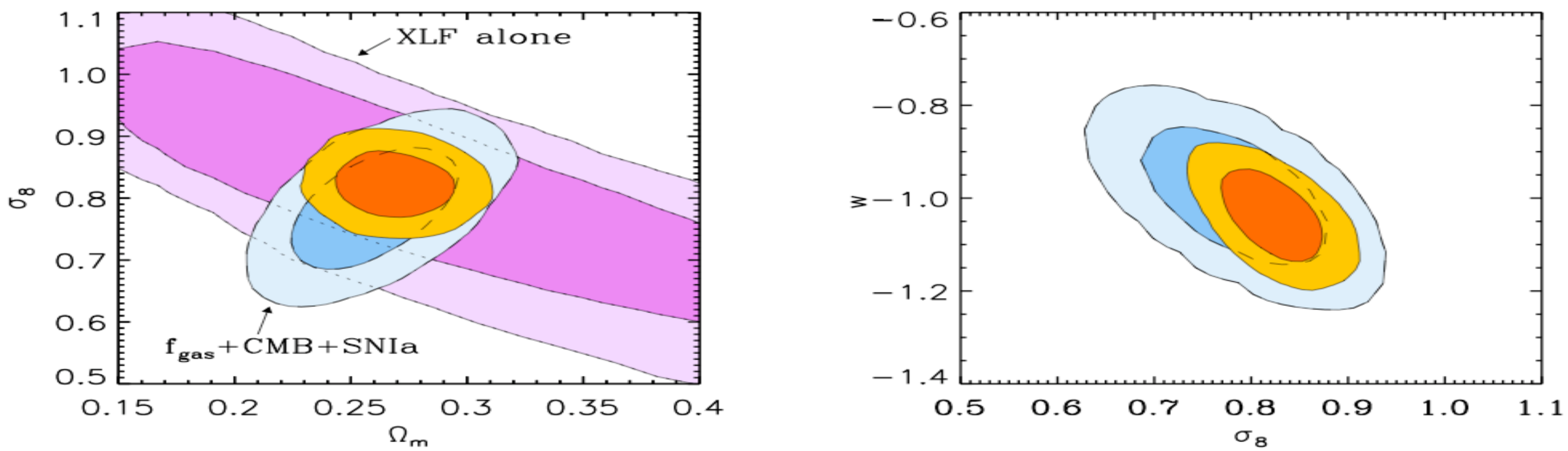

Figure 10. Joint 68.3 and 95.4 per cent confidence constraints on Ω_m and σ_8 (left) and σ_8 and w (right) obtained from a combined f_{gas}+CMB+SNIa analysis (blue) and the improved constraints obtained by combining these data with the XLF (gold). No priors on h, $\Omega_b h^2$ or n_s are imposed in either analysis. In the left panel, the results from the XLF alone using standard priors (Table 1) are shown (purple) in order to illustrate the degeneracy breaking.

Dark Energy Task Force '07

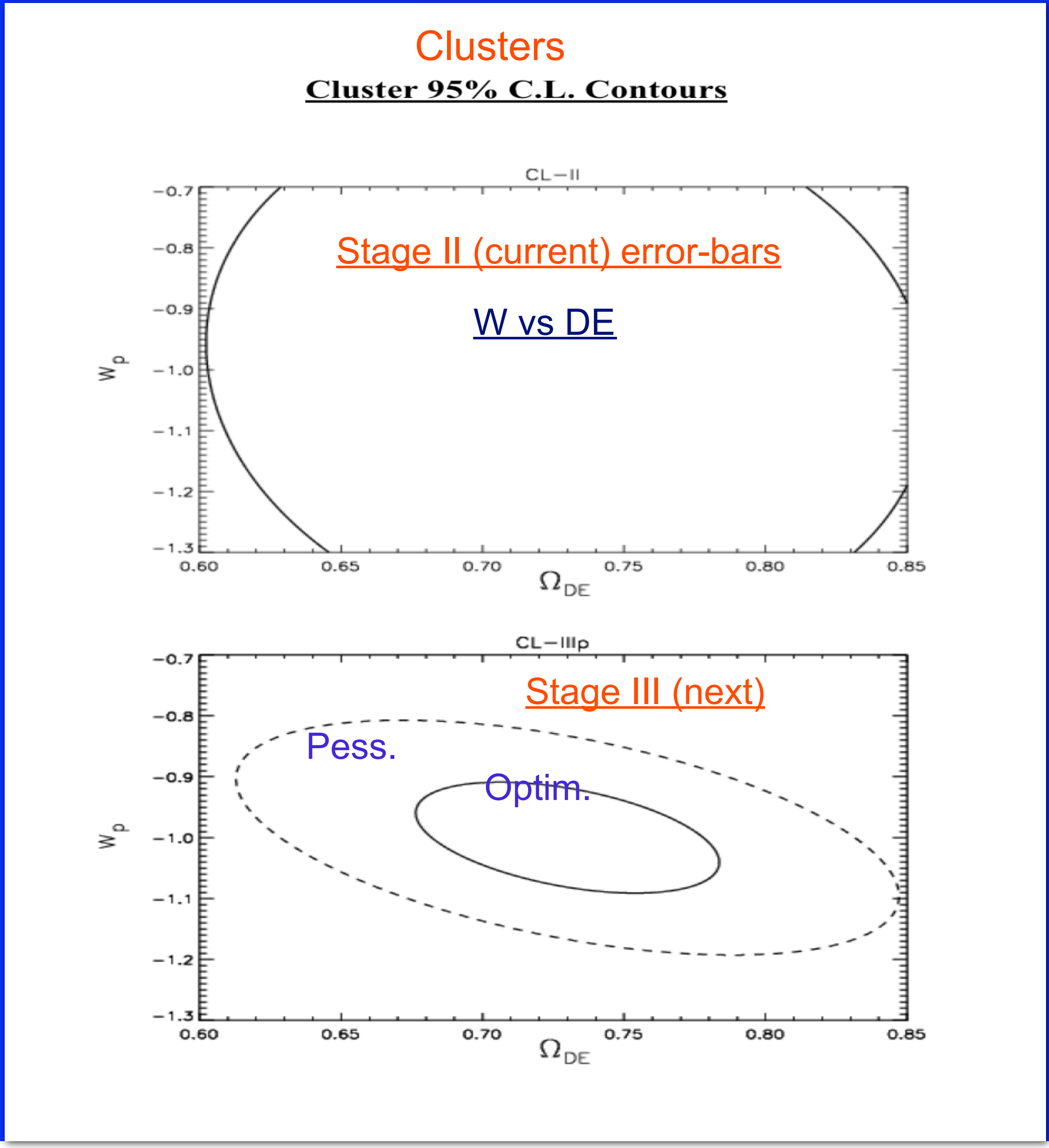

Dark Energy Task Force: Stage-3 Comparison

the large degree of uncertainty due to uncertain forecasts of systematic errors.

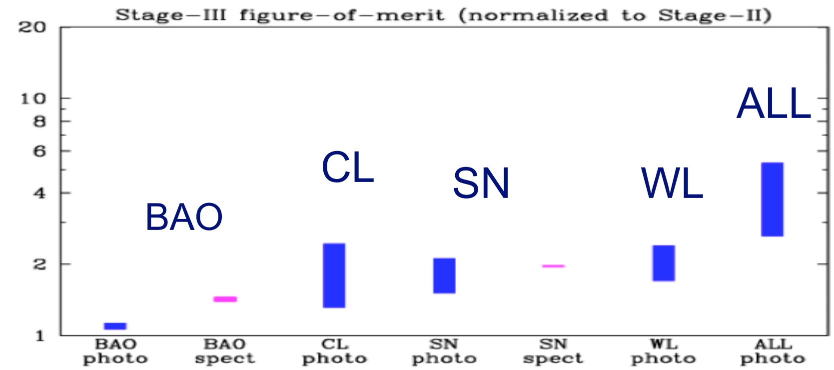

Illustration of the potential improvement in the DETF figure of merit arising from Stage III projects. The improvement is given for the different techniques individually, along with various combinations of techniques. In the figure 'photo' and 'spect' refers to photometric and spectroscopic surveys, respectively. Each bar extends from the expectation with pessimistic systematics up to the expectation with optimistic systematics. "ALL photo" combines photometric survey results from BAO, CL, SN, and WL.

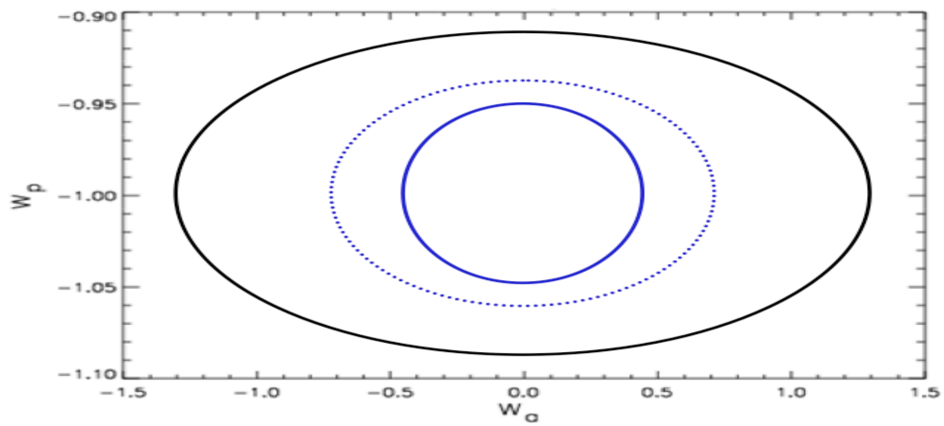

Illustration of the potential improvement in the DETF figure of merit arising from Stage III projects in the w_a–w_p plane. The DETF figure of merit is the reciprocal of the area enclosed by the contours. The outer contour corresponds to Stage II, and the inner contours correspond to pessimistic and optimistic ALL-photo. All contours are 95% C.L.

Dark Energy Task Force: Stage-4 Comparison (Space)

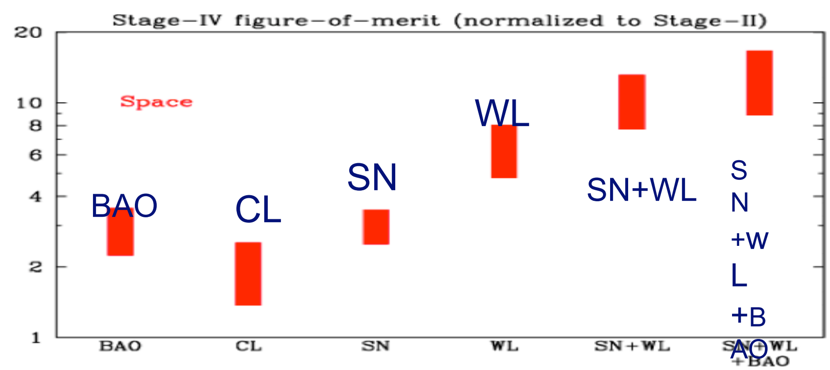

Illustration of the potential improvement in the DETF figure of merit arising from Stage IV space-based projects. The bars extend from the pessimistic to the optimistic projections in each case. The final two error bars illustrate the improvement available from combining techniques; other combinations of techniques may be superior or more cost-effective. CL results are from an x-ray satellite; the others results from an optical/NIR satellite.

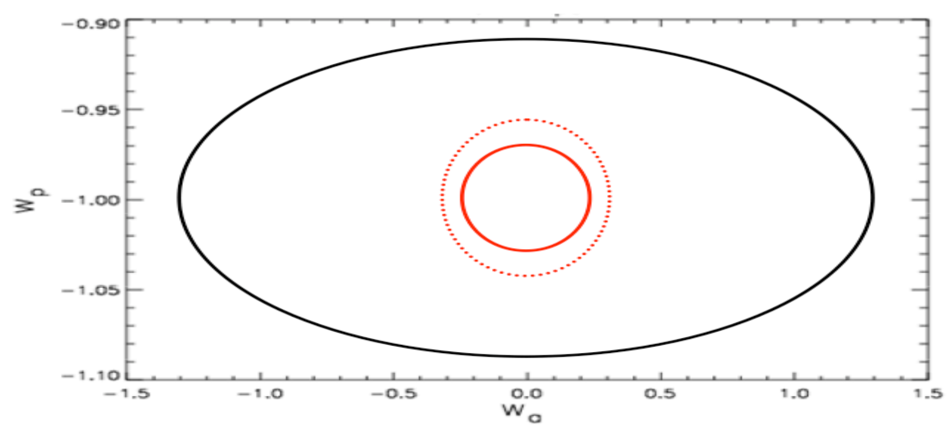

Illustration of the potential improvement in the DETF figure of merit arising from Stage IV space-based projects in the w_a–w_p plane. The DETF figure of merit is the reciprocal of the area enclosed by the contours. The outer contour corresponds to Stage II, and the inner contours correspond to pessimistic and optimistic BAO+SN+WL. All contours are 95% C.L.

DETF: Compare All (Stage 4: space+ground)

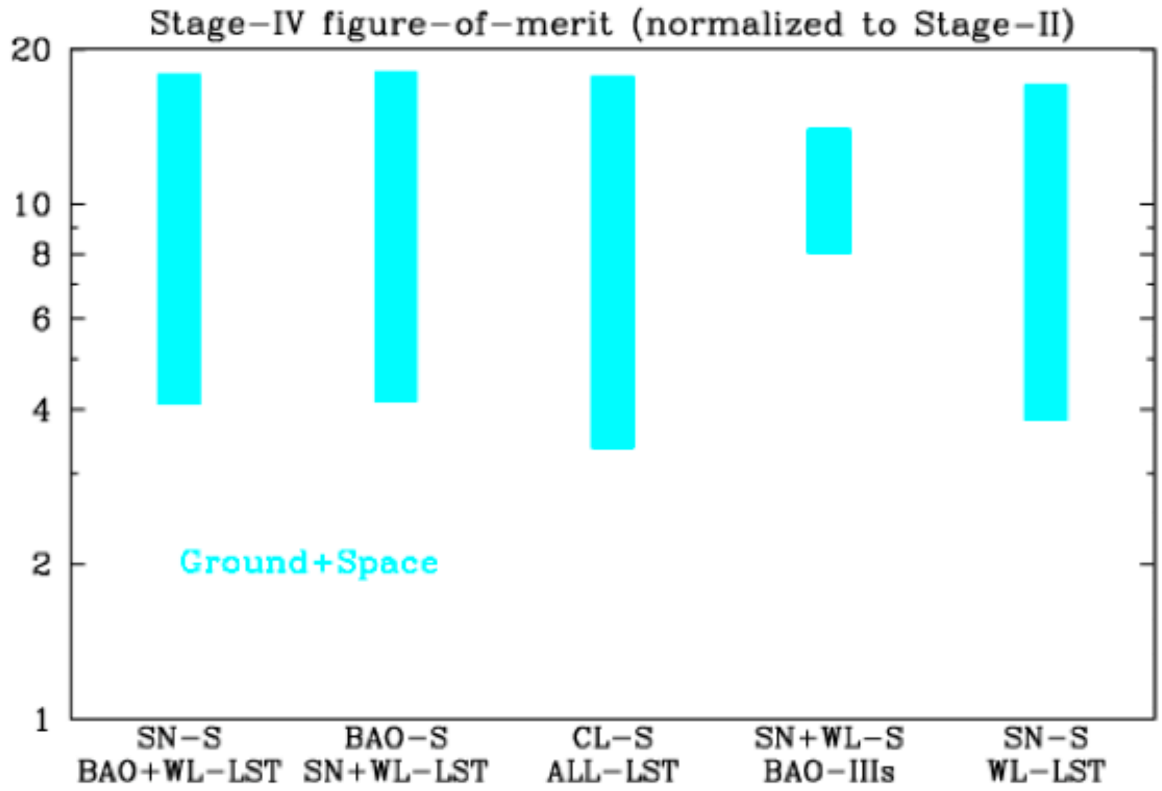

This figure illustrates the potential improvement in the DETF figure of merit arising from a combination of Stage IV space-based and ground-based projects. The bars extend from the pessimistic to the optimistic projections in each case. This is by no means an exhaustive search of possible ground/space combinations, just a representative sampling to illustrate that uncertainties on each combination are as large as the differences among them.

Cluster Method: DETF

- Strong statistical benefits
- Largest systematic errors (vs. SN, BAO, WL?)
- Need to control systematics due to non-linear astrophysical processes (baryon physics; baryon evolution; ICM -- heating, cooling, non-thermal, merging…)
- Need accurate and reliable Mass calibration

  (accurate comparisons of lensing, X-ray, SZ, Opt, and sims.)

- Clusters: Important method when combined with SN or BAO (which measure only d(z)), in order to test both D.E. and GR (CL and WL measure both d(z) and gravitational growth)

Ω_m from Baryon Fraction

- $\Omega_b/\Omega_m = 0.18 +- 0.02$ *h=0.7*
  (Clusters; CMB)

- $\Omega_b = 0.042 +- 0.004$ *(BBN; CMB)*

→ $\Omega_m = 0.24 +- 0.04$

Baryon Fraction vs. Scale *(→ 0.18)*

(Bahcall & Martin '07)

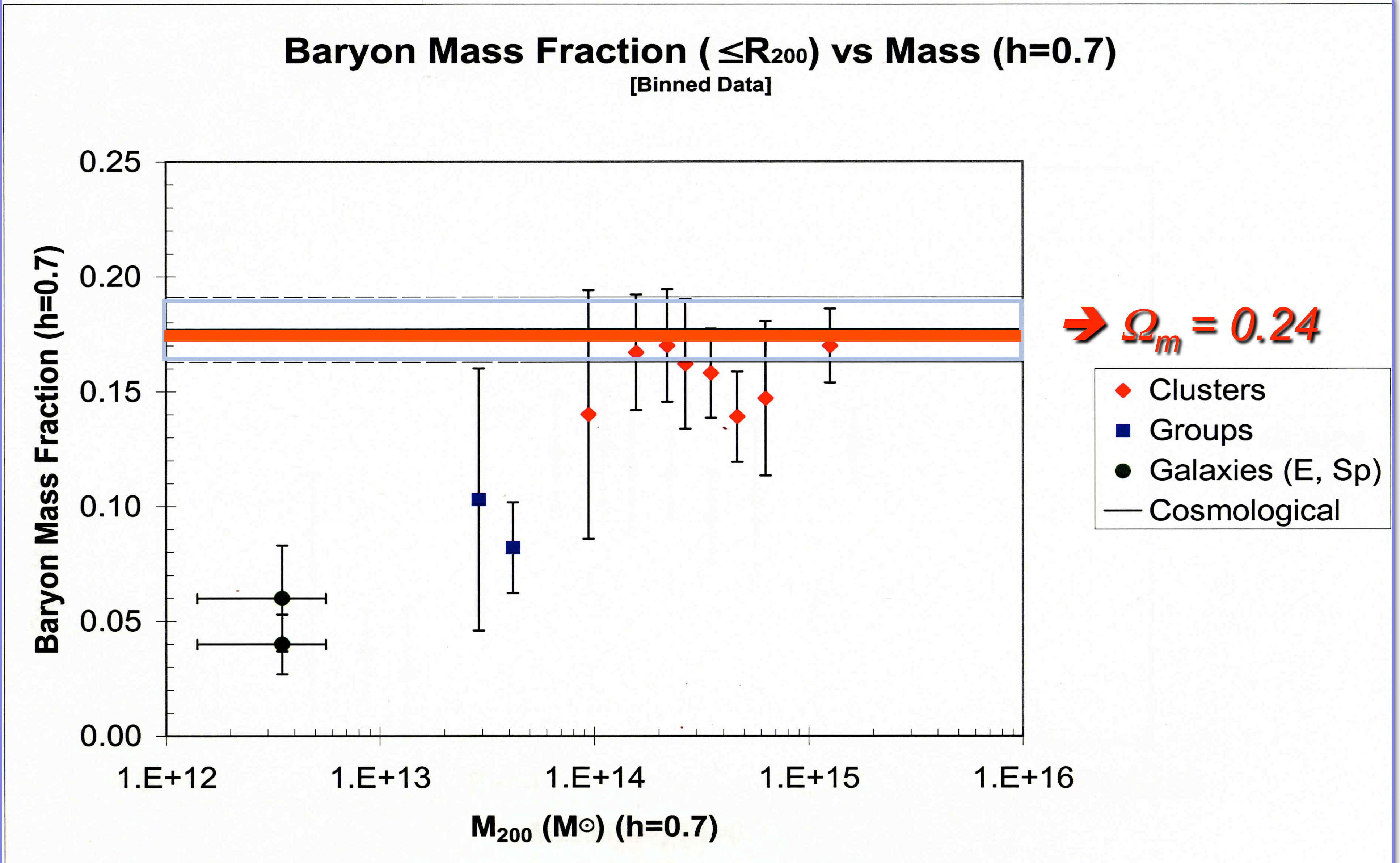

Evolution of Cluster Gas Fraction

(Allen et al 07)

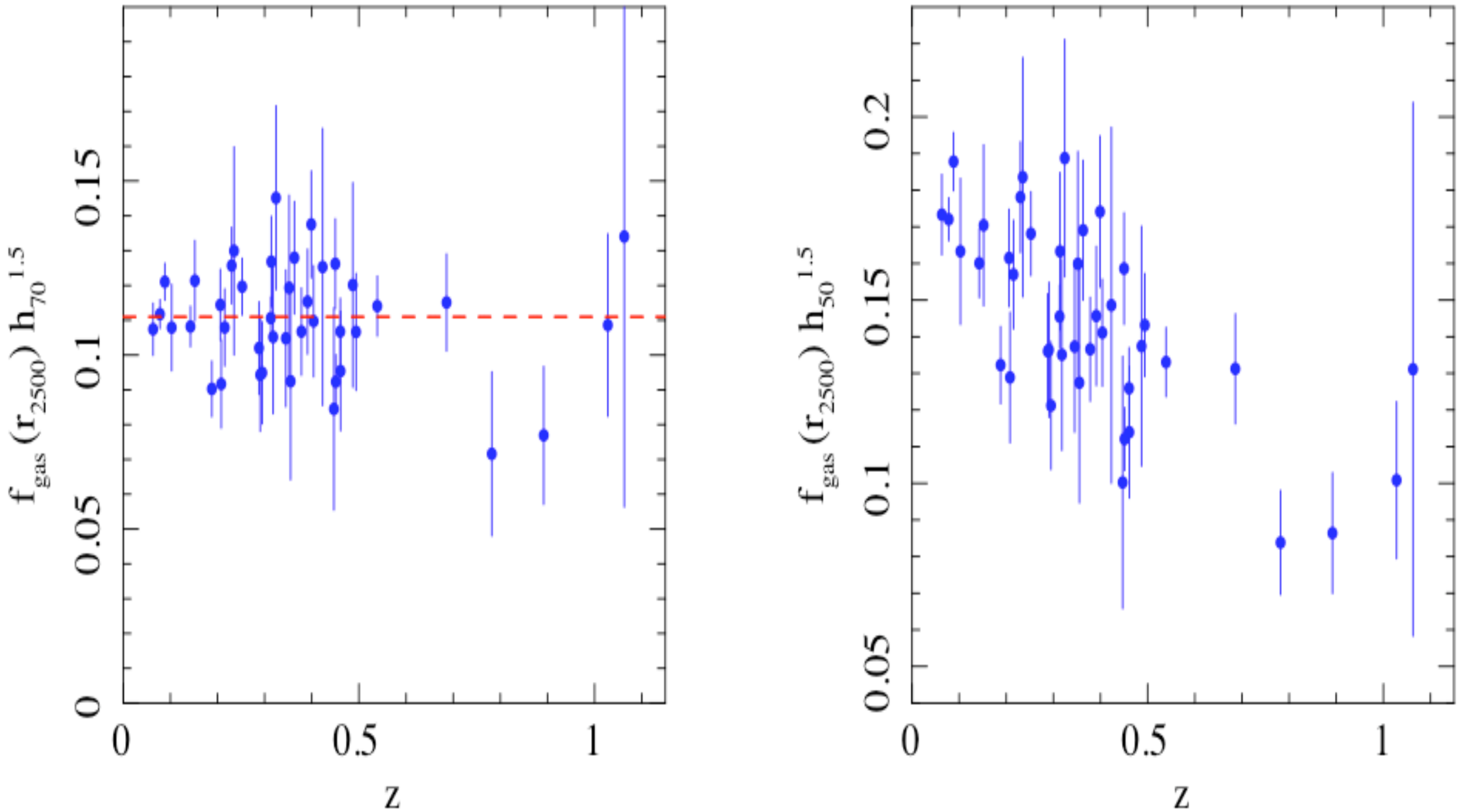

Figure 2. The apparent variation of the X-ray gas mass fraction measured within r_{2500} as a function of redshift for the (a: left panel) reference ΛCDM and (b: right panel) reference SCDM ($\Omega_{\rm m} = 1.0$, $\Omega_\Lambda = 0.0$, $h = 0.5$) cosmologies. The plotted error bars are statistical root-mean-square 1σ uncertainties. The global, absolute normalization of the $f_{\rm gas}$ value should be regarded as uncertain at the $\sim 10-15$ per cent level due to systematic uncertainties in instrument calibration, modelling and the level of non-thermal pressure support (Section 4.2).

Cosmology: Evolution of Gas Fraction
(Allen 07)

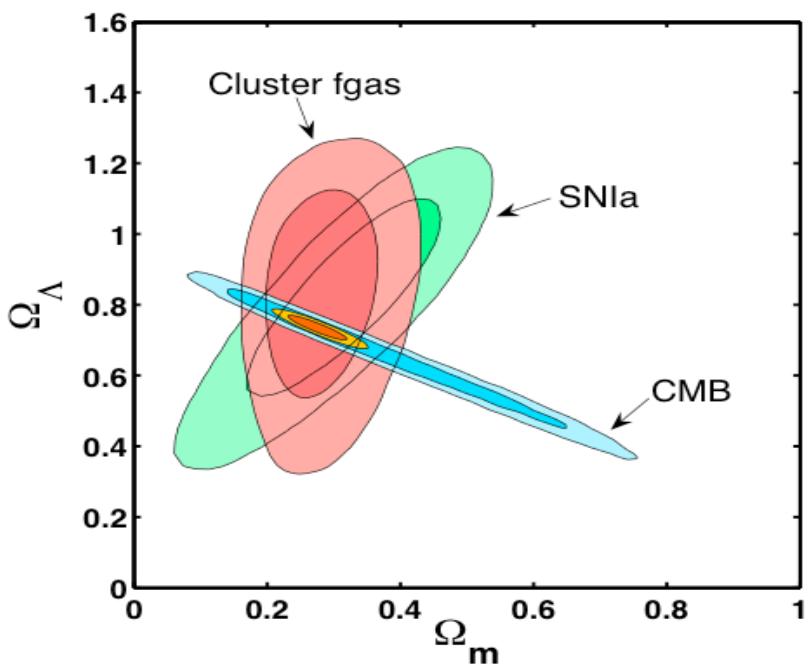

Figure 6. The 68.3 and 95.4 per cent (1 and 2 σ) confidence constraints in the $\Omega_{\rm m}, \Omega_\Lambda$ plane for the Chandra $f_{\rm gas}$ data (red contours; standard priors on $\Omega_{\rm b}h^2$ and h are used). Also shown are the independent results obtained from CMB data (blue contours) using a weak, uniform prior on h ($0.2 < h < 2$), and SNIa data (green contours; the results for the Davis *et al.* 2007 compilation are shown). The inner, orange contours show the constraint obtained from all three data sets combined (no external priors on $\Omega_{\rm b}h^2$ and h are used). A ΛCDM model is assumed, with the curvature included as a free parameter.

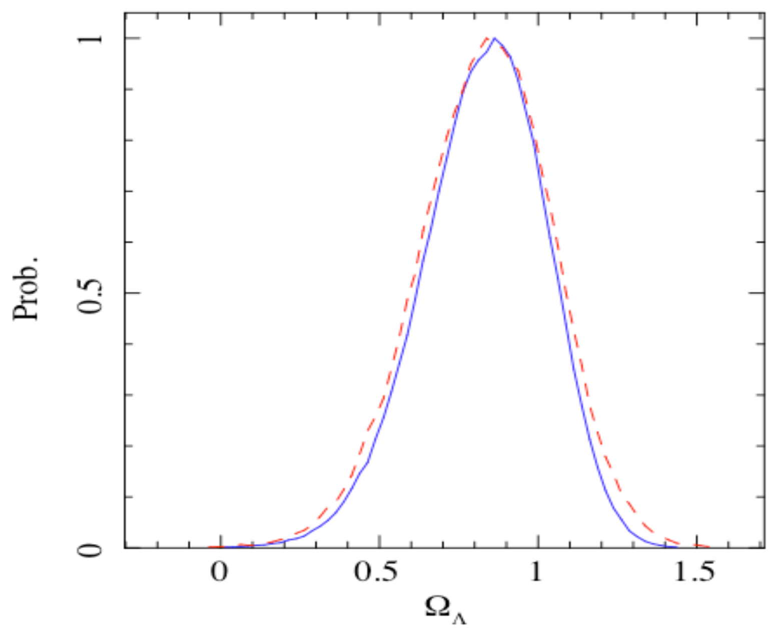

Figure 7. The marginalized constraints on Ω_Λ determined from the Chandra $f_{\rm gas}$ data using the non-flat ΛCDM model and standard (solid curve) and weak (dashed curve) priors on $\Omega_{\rm b}h^2$ and h. The $f_{\rm gas}$ data provide a detection of the effects of dark energy at the ~ 99.99 per cent confidence level.

$\Omega_\Lambda = 0.735 \pm 0.023$. Together, the $f_{\rm gas}$+CMB+SNIa data also constrain the Universe to be close to geometrically flat: $\Omega_{\rm k} = -0.010 \pm 0.011$. No external priors on $\Omega_{\rm b}h^2$ and h are used in the analysis of the combined $f_{\rm gas}$+CMB+SNIa data (see also Section 5.6).

Finally, we have examined the effects of doubling the allowance for non-thermal pressure support in the clusters

Comlogical constraints from Gas Fraction

(Allen etal 07)

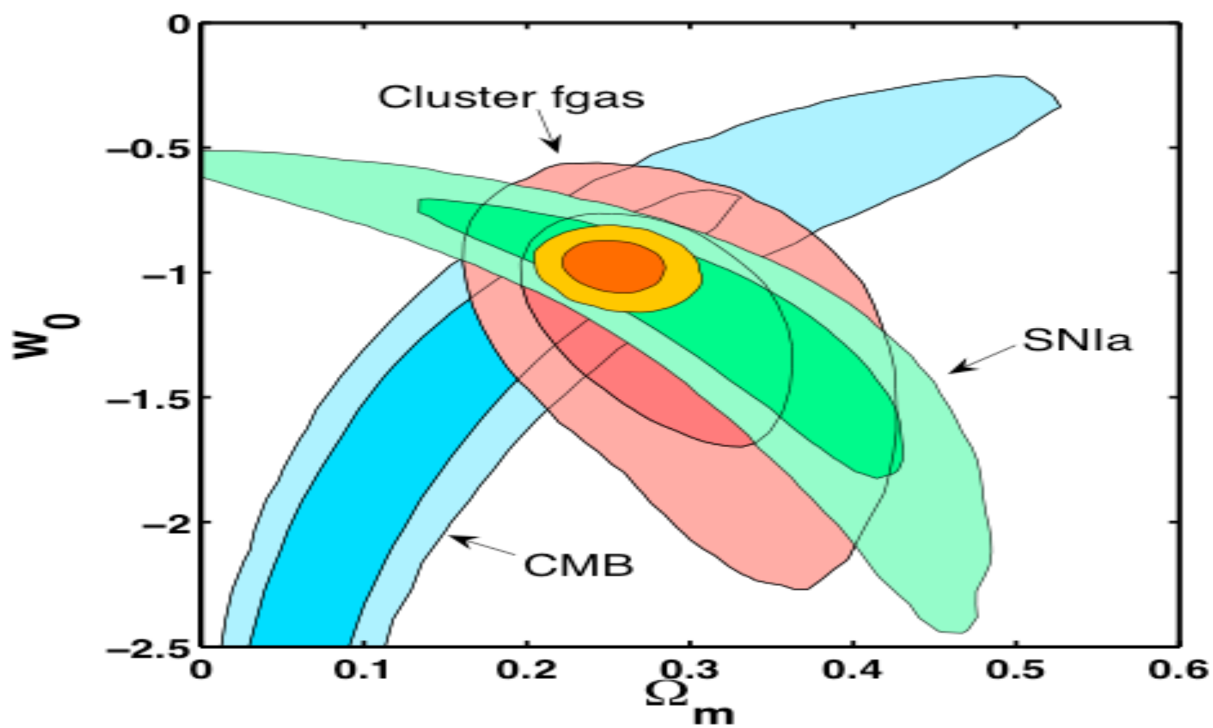

Figure 8. The 68.3 and 95.4 per cent (1 and 2σ) confidence constraints in the Ω_m, w plane obtained from the analysis of the Chandra f_{gas} data (red contours) using standard priors on $\Omega_b h^2$ and h. Also shown are the independent results obtained from CMB data (blue contours) using a weak, uniform prior on h ($0.2 < h < 2.0$) and SNIa data (green contours; Davis *et al.* 2007). The inner, orange contours show the constraint obtained from all three data sets combined: $\Omega_m = 0.253 \pm 0.021$ and $w = -0.98 \pm 0.07$ (68 per cent confidence limits). No external priors on $\Omega_b h^2$ and h are used when the data sets are combined. A flat cosmology with a constant dark energy equation of state parameter w is assumed.

Baryon Acoustic Oscillations: SDSS

(Eisensteain etal 05)

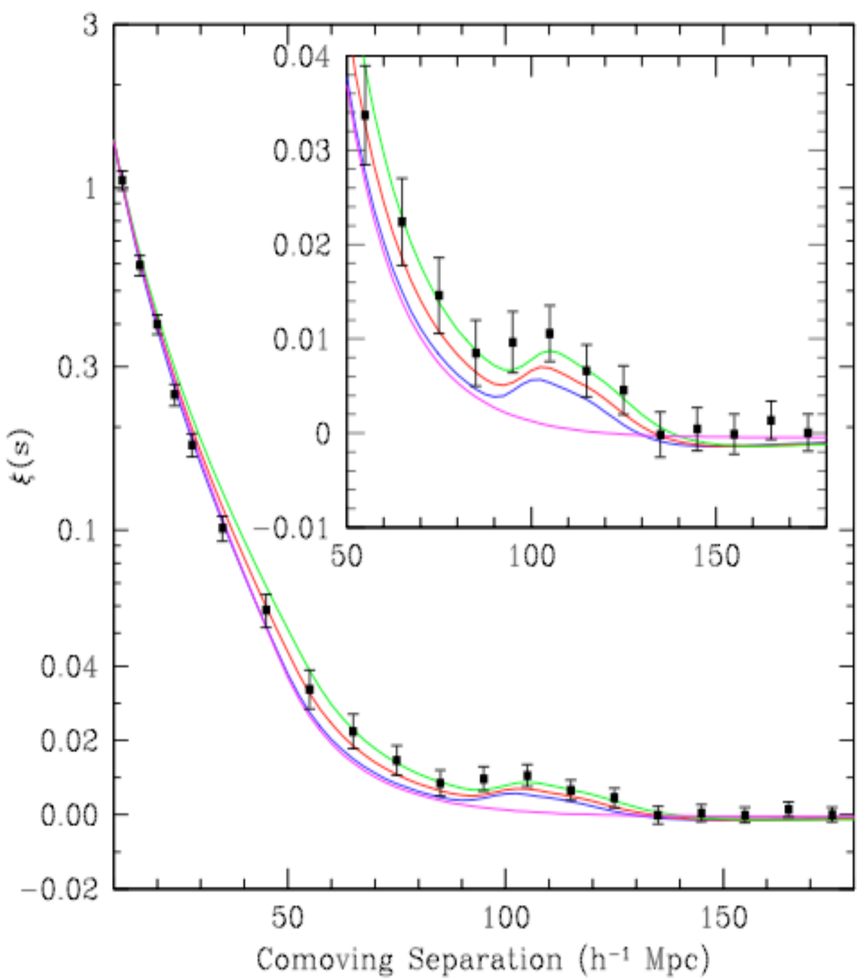

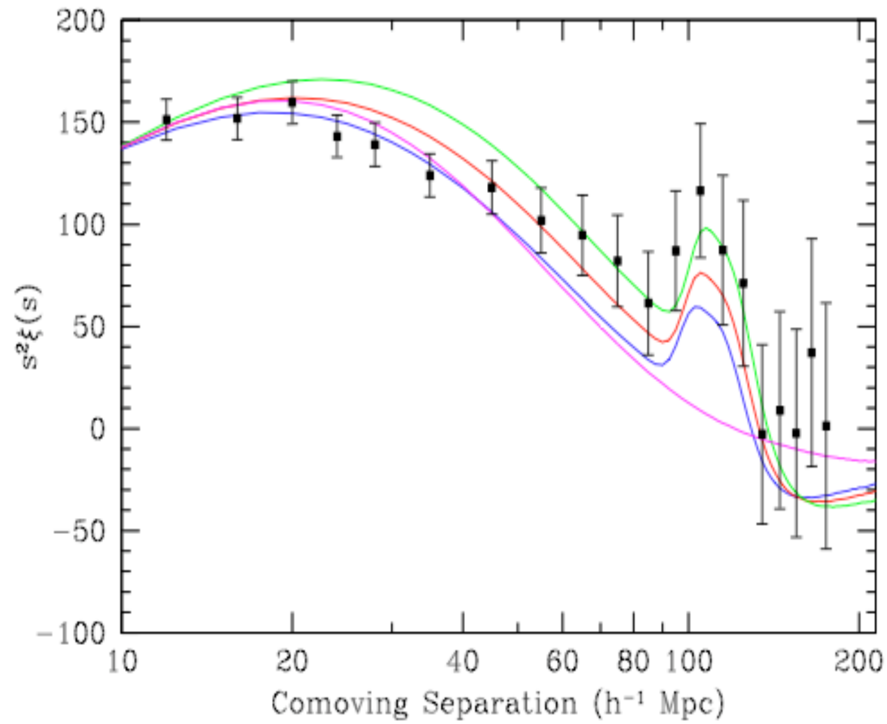

FIG. 3.— As Figure 2, but plotting the correlation function times s^2. This shows the variation of the peak at $20h^{-1}$ Mpc scales that is controlled by the redshift of equality (and hence by $\Omega_m h^2$). Varying $\Omega_m h^2$ alters the amount of large-to-small scale correlation, but boosting the large-scale correlations too much causes an inconsistency at $30h^{-1}$ Mpc. The pure CDM model (magenta) is actually close to the best-fit due to the data points on intermediate scales.

FIG. 2.— The large-scale redshift-space correlation function of the

BAO: Cluster Correlation Function

(Bahcall and Soneira 1983)

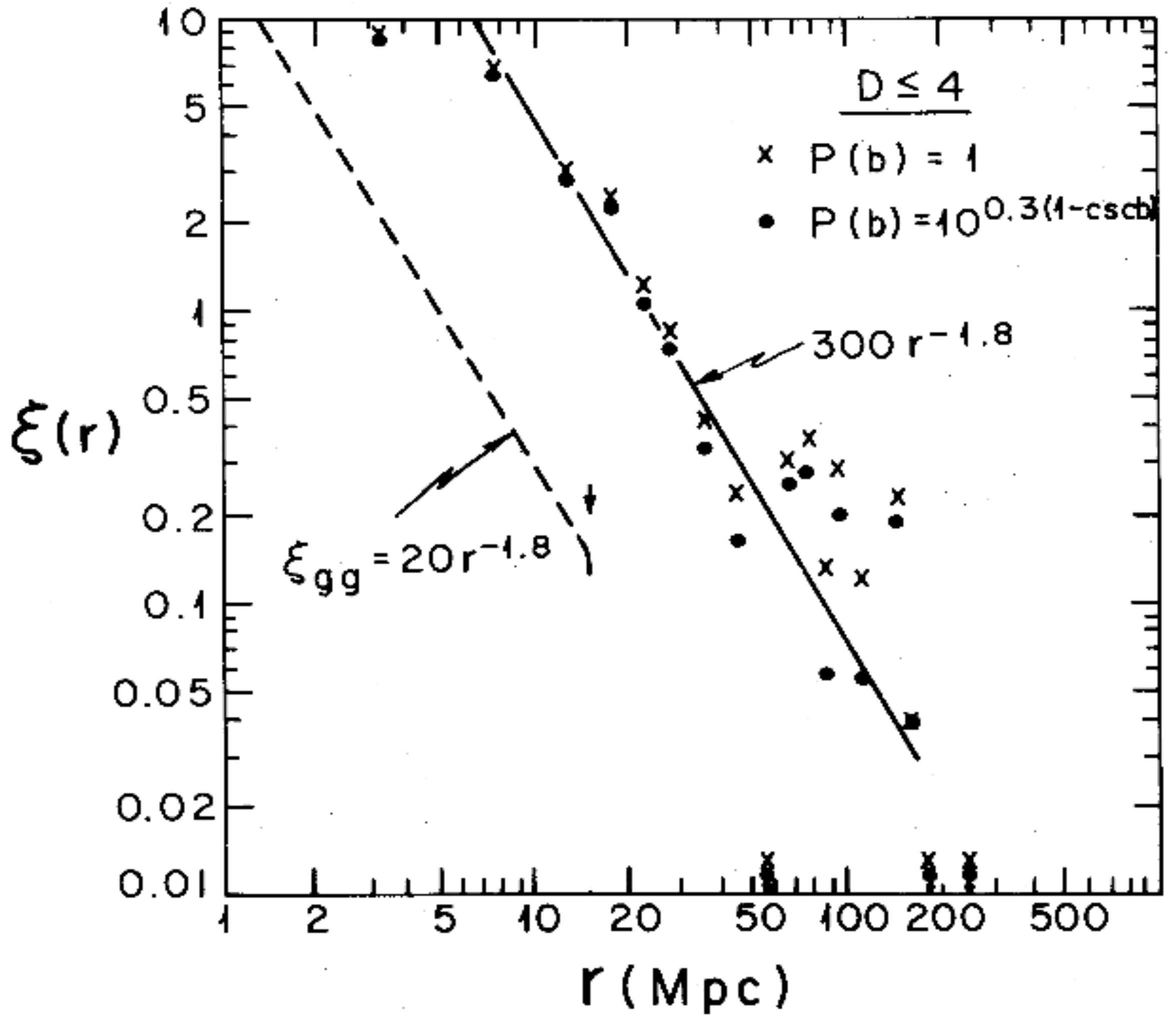

FIG. 9a

BAO: Cluster Correlation Function

(Bahcall and Soneira 1983)

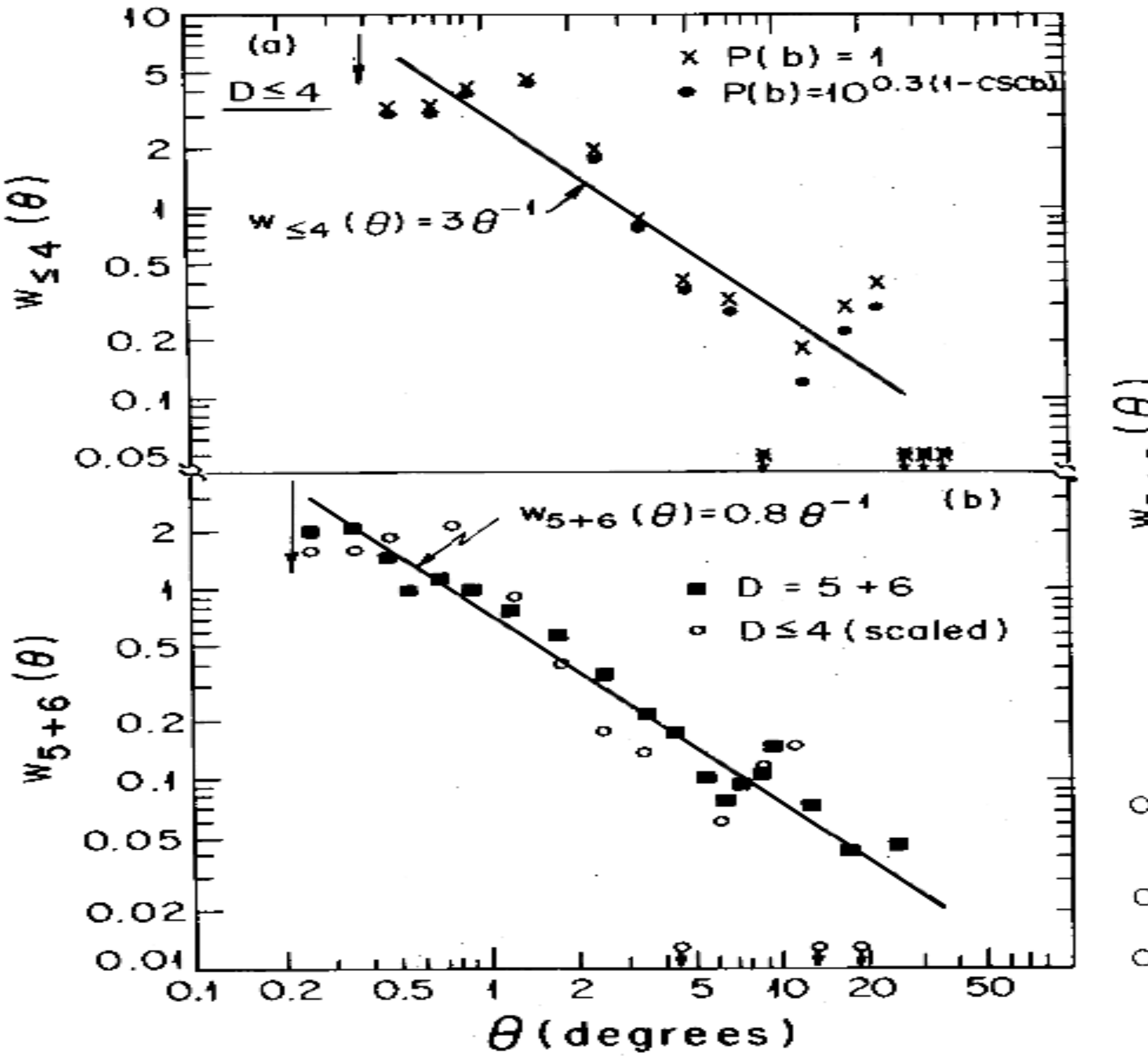

FIG. 5a, b

Shape and Alignment of Clusters

- The Shape of Clusters
- Alignment of Cluster Pairs
- Evolution of Shape & Alignment
- New Tool in Cosmology:

  → ***Cluster Ellipticity***

Evolution of Cluster Ellipticity

<E> versus Redshift and Mass (Hopkins, Bahcall, etal '05)

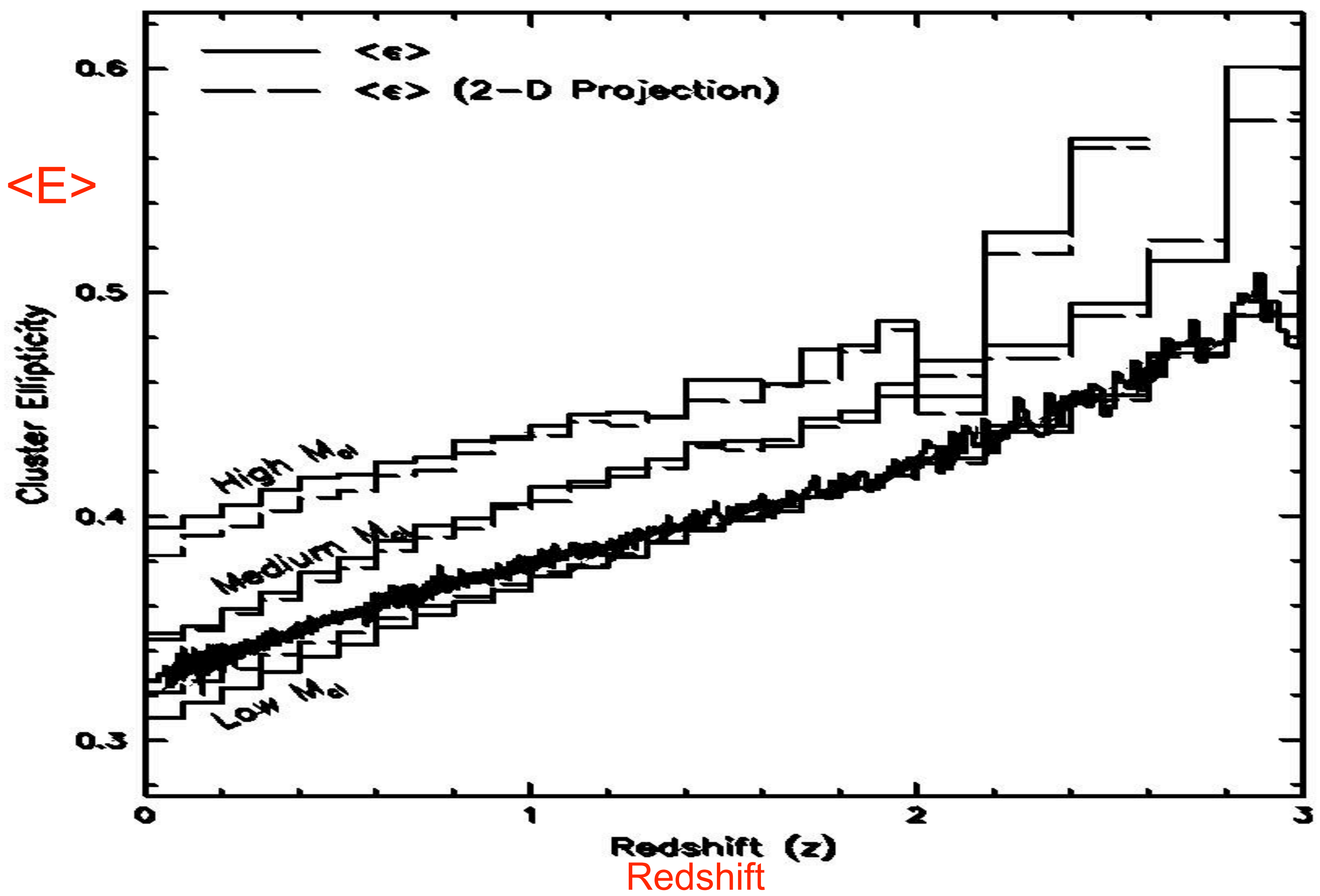

Cluster Ellipticity → σ_8

(Ho, Bahcall, Bode '06)

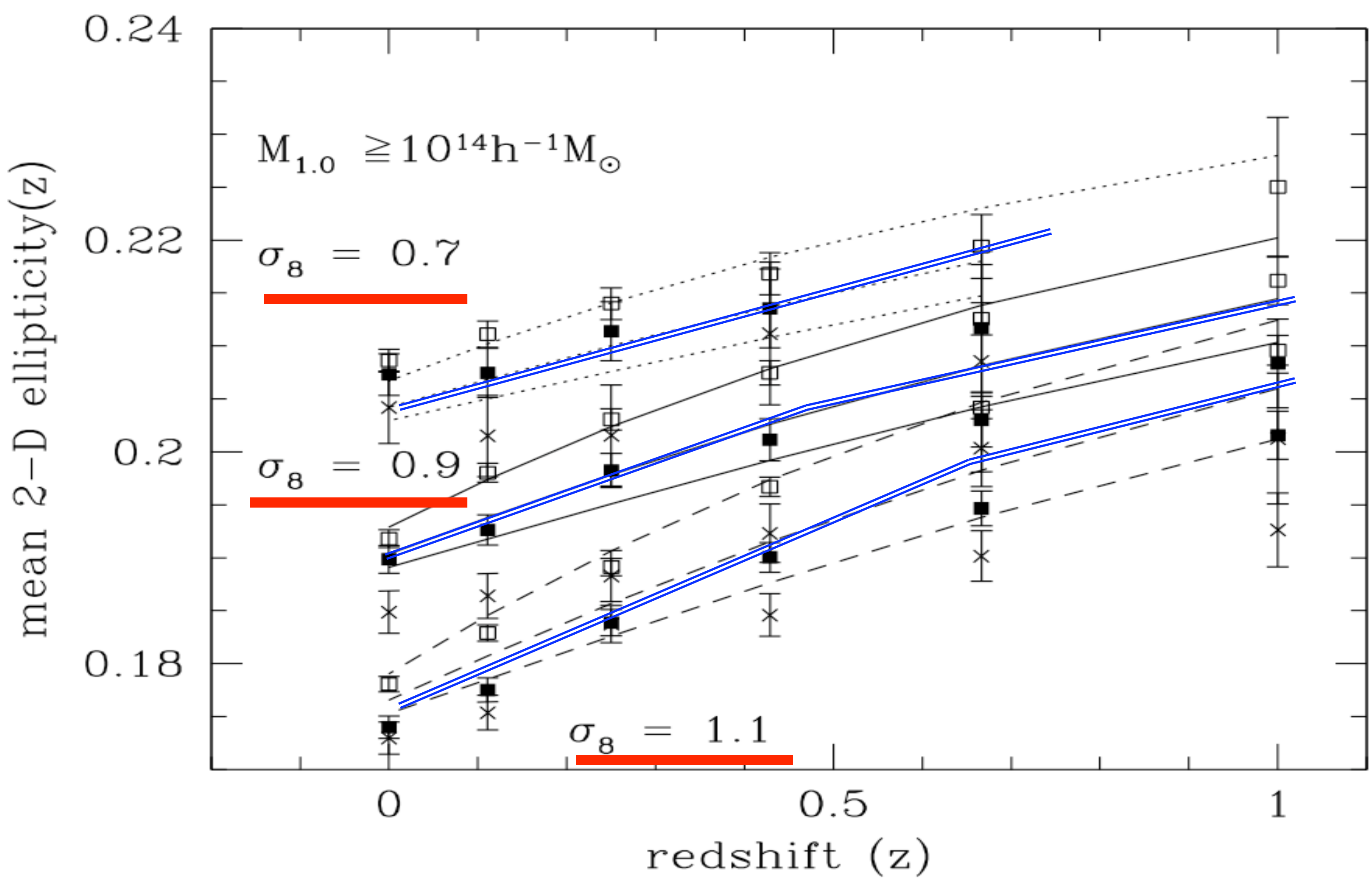

Clusters Shape and Alignment

- Clusters are *Triaxial*
  - > More so at earlier times
- $<E_{cl}> \sim 0.3$ to 0.5 (z ~ 0 to 3)

(ellipticity causes selection bias: opt, lensing, X-ray; need to account for it)

- Strong Cluster *Alignment to ~100 Mpc*
- Alignment and Ellipticity *increase with z*
- *New Tool in Cosmology:*

$$<E_{cl}> \rightarrow \sigma_8 \quad \Omega_m \quad w$$

Clusters: Tool for LSS, Structure Formation and Evolution, ICM physics and evolution

- Large Scale Structure (CF, Pk, SCs)
- Evolution of baryon fraction; gas vs. gal
- ICM Physics; Cooling, heating, AGNs, non-thermal, merging and shocks, winds, metalicities, evolution
- Substructure; merging clusters; high-velocity mergers (e.g., Bullet Cluster)
- Soft - hard excess emission in clusters
- Ellipticity and alignment of clusters vs. z

The Warm Universe (10^5-10^7)

- Where are ~50% of the baryons?
- Define 'WHIM' better (e.g. diffuse and bound/groups?) how best look for it -- use different methods, emission, absorption, targeted SCs, …; Are most in Groups?
- Tracing the IGM, SCs/filaments, galactic halos
- Evolution of the warm IGM and its LSS; Physics of the Warm IGM
- Cosmology: comparison with LCDM

Superclusters: Filaments or Pancakes?
(Wray, Bahcall, Bode, etal '06)

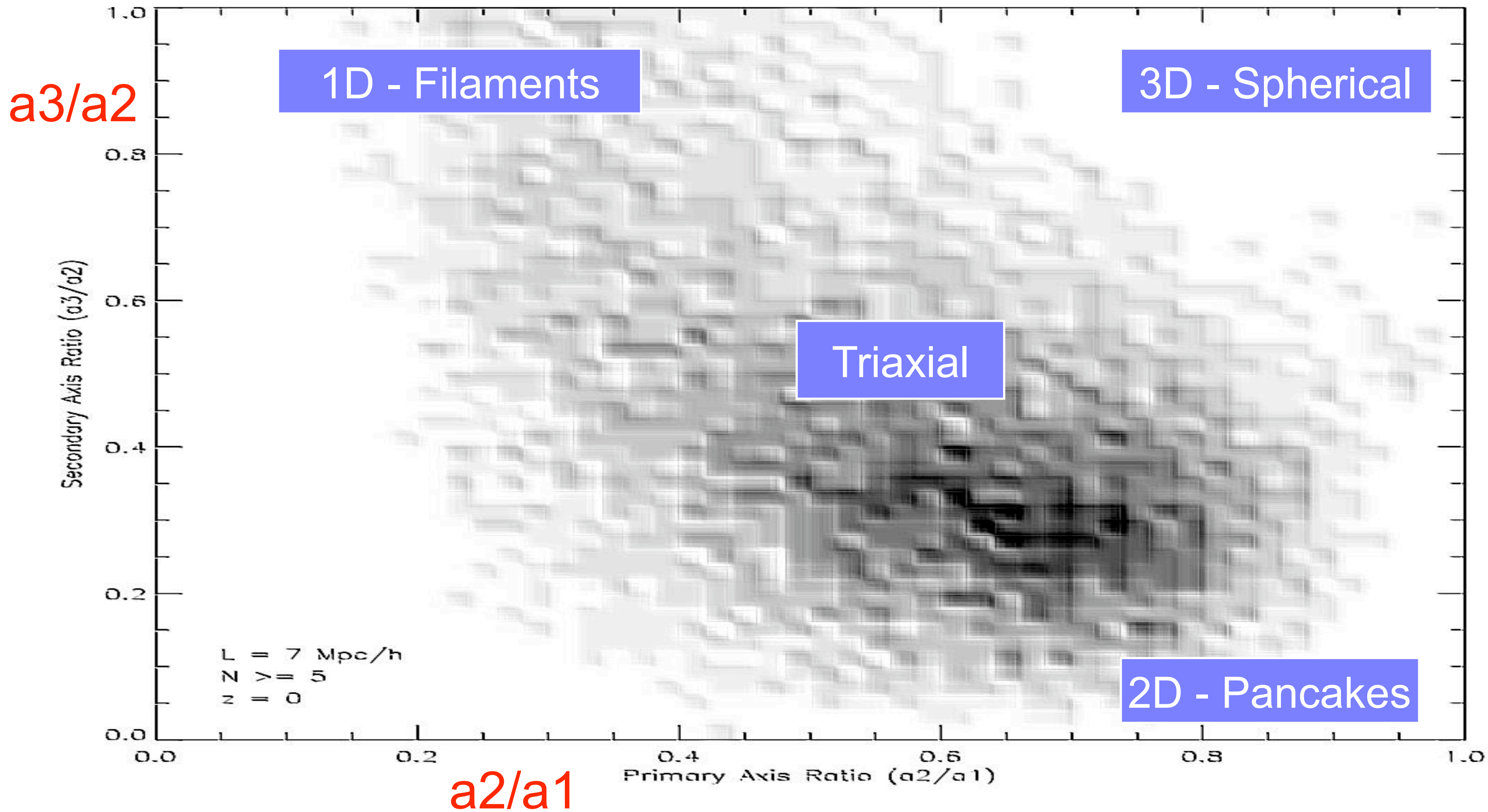

Fig. 9.— Bivariate distribution of primary and secondary axis ratios for low-z superclusters found with linking length $L = 7h^{-1}$ Mpc. See the text (§3.4) for interpretation.

Summary

The Hot Universe: Clusters

- Powerful tool for Cosmology (Ω_m Ω_Λ σ_8 ω)
- Need accurate Mass calibration and baryon/ICM physics and evolution!
- Powerful tool for Tracing Large Scale Structure (Pk, SCs, BAO)
- Structure Formation and Growth; ICM physics & Evolution

The Warm Universe: IGM

- Where are all the baryons? Use variety methods to search
- Tracing the IGM and Large-scale Structure; Physics of WHIM
- Cosmology: compare with expectations

Test MOND

The End

Many thanks to Frits, Richard Lieu and all the organizers of this fruitful and enjoyable meeting!

Good Luck and good progress in the

Warm-Hot Universe

Mass-to-Light Function

(Bahcall, Lubin & Dorman '95; Bahcall and Fan '98)

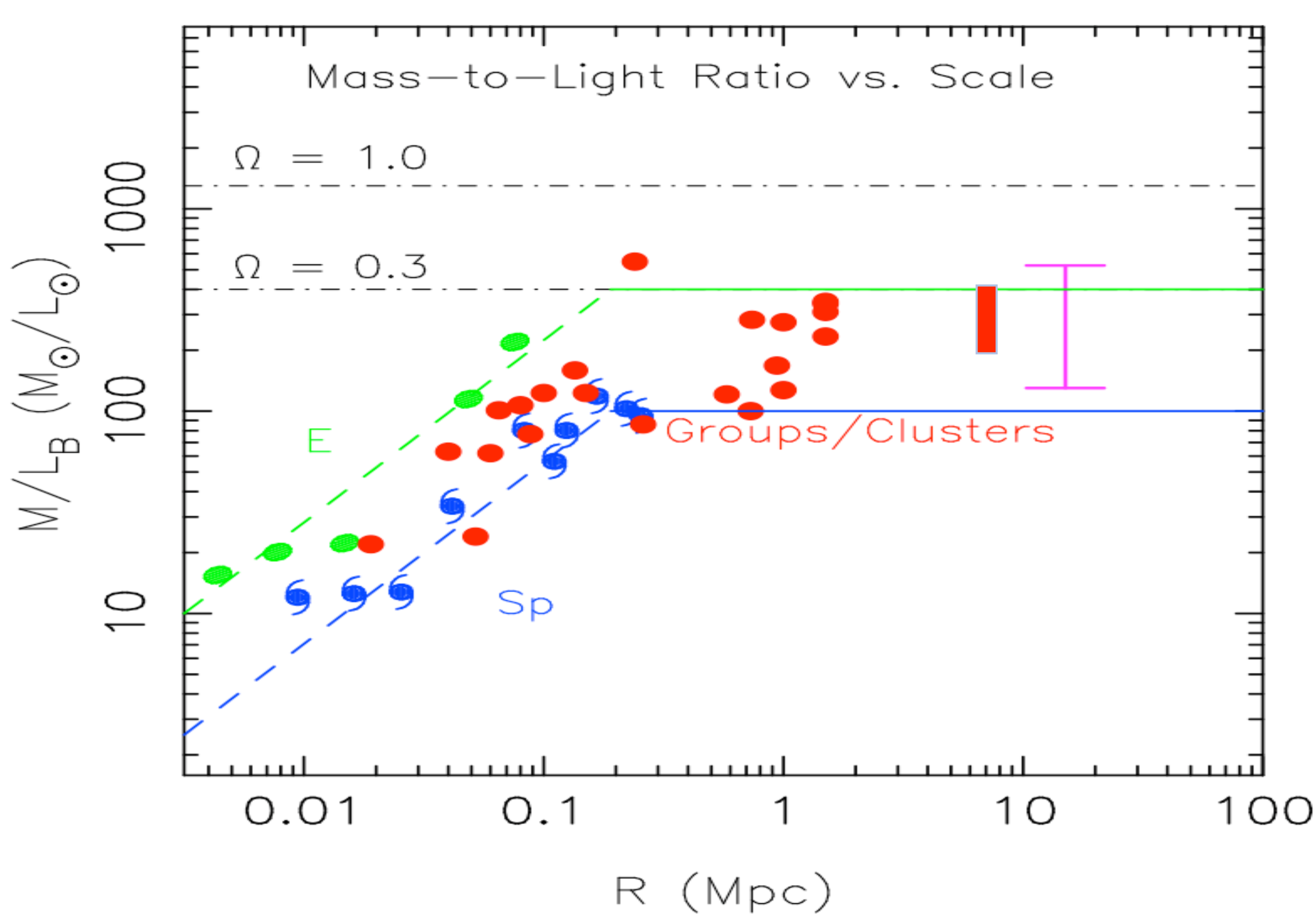

Cluster M/L Function from SDSS

(Sheldon et al 07)

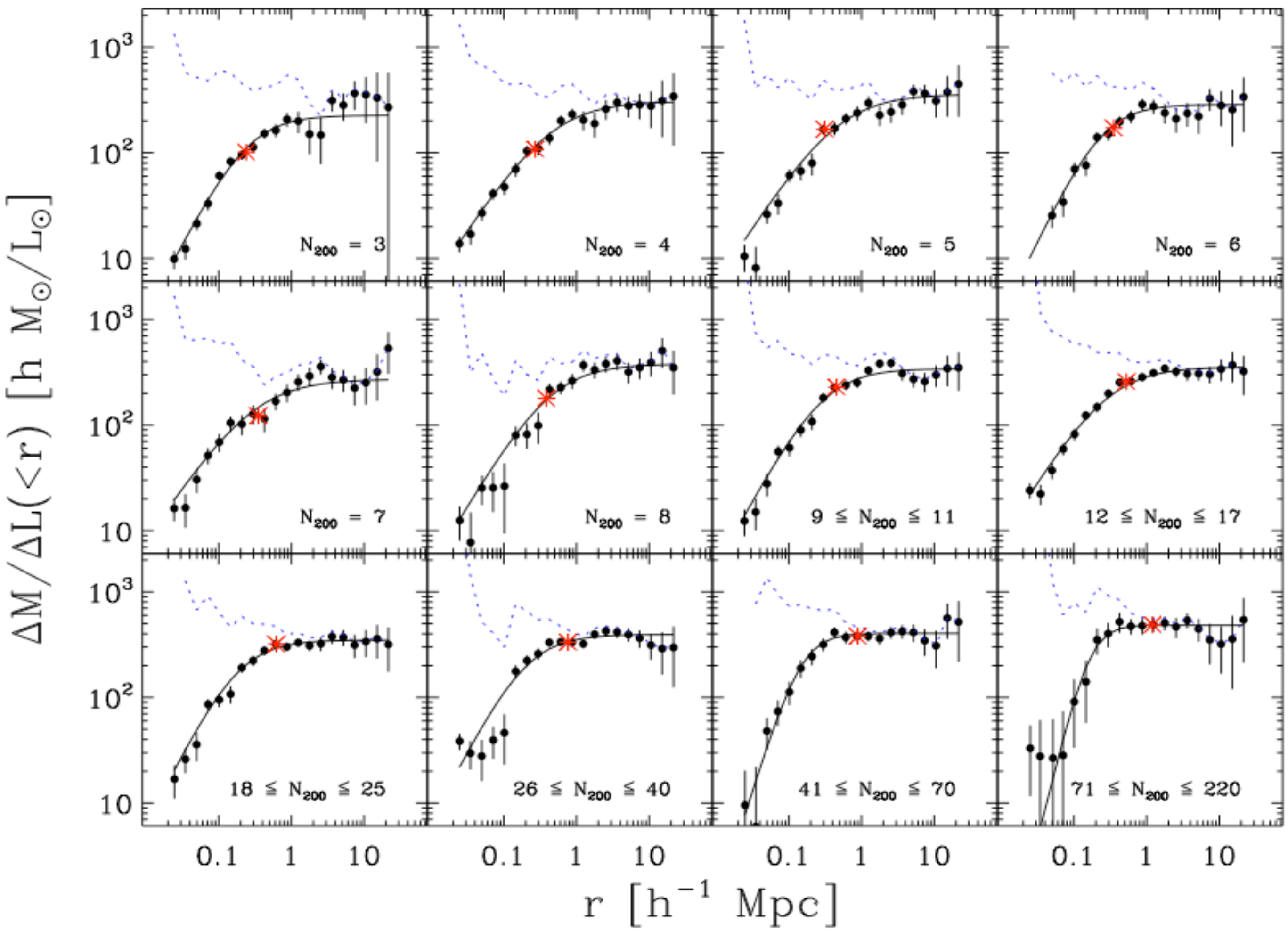

FIG. 8.— Excess mass to excess light ratio profiles for each of the N_{200} bins. Light is measured in the $^{0.25}i$ bandpass. These curves are the ratio of the curves shown in Figures 6 and 7. The points with error bars include the mean BCG luminosity, while the dotted curves exclude the luminosity of the BCG. The asterisk marks r_{200}^{mass}. The curve through the data is a simple descriptive model as discussed in §8.6.

Cluster M/L : SDSS

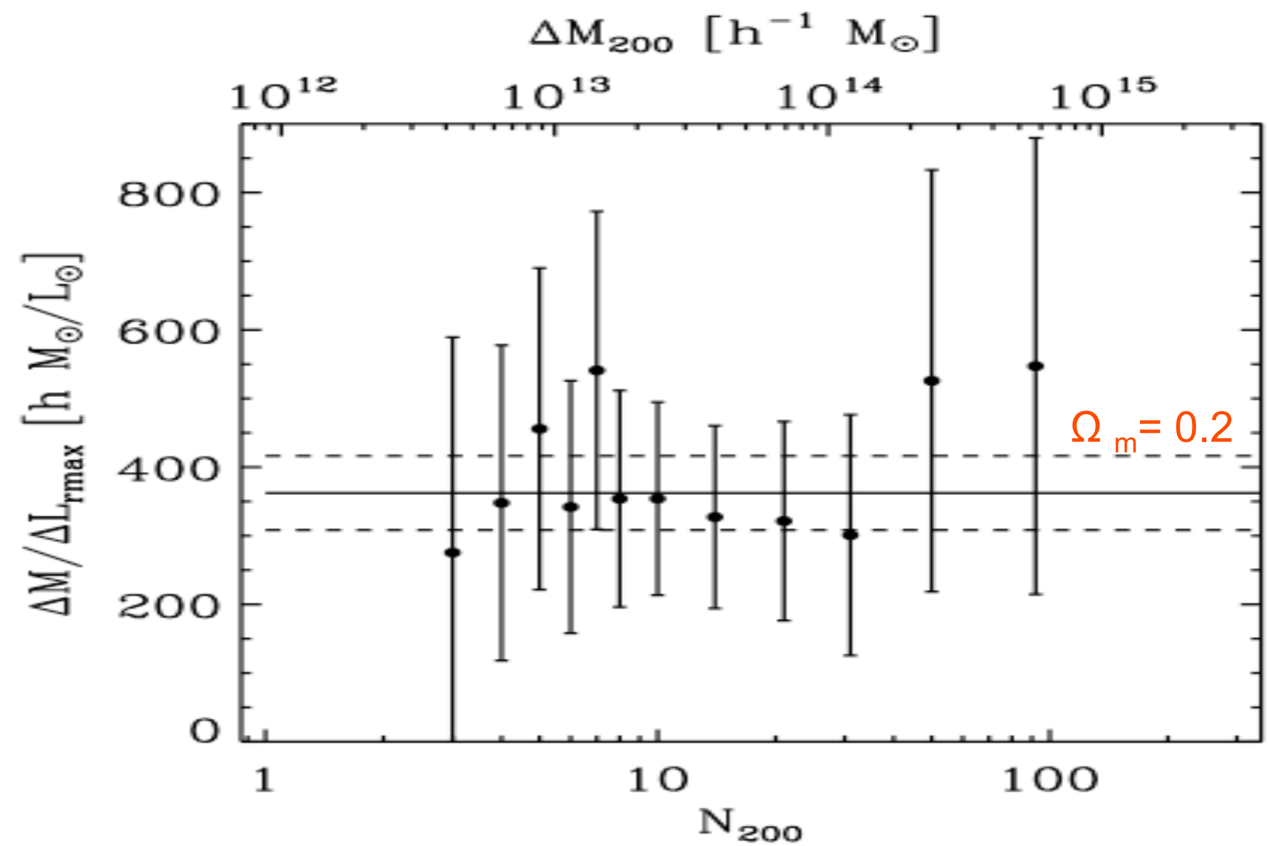

FIG. 10.— Asymptotic excess mass-to-light ratio as a function of N_{200}. Light is measured in the $^{0.25}i$ bandpass. This is simply the last point on the integrated $\Delta M/\Delta L$ curve at $r = 22h^{-1}$Mpc. The mean ΔM within r_{200}^{mass} centered on BCGs is shown on the top axis, although this is only rough since the transformation between N_{200} and mass is non-linear. The mean $\Delta M/\Delta L = 362 \pm 54h$, averaged over all samples, is plotted as the horizontal line

Dark Energy Task Force: BAO

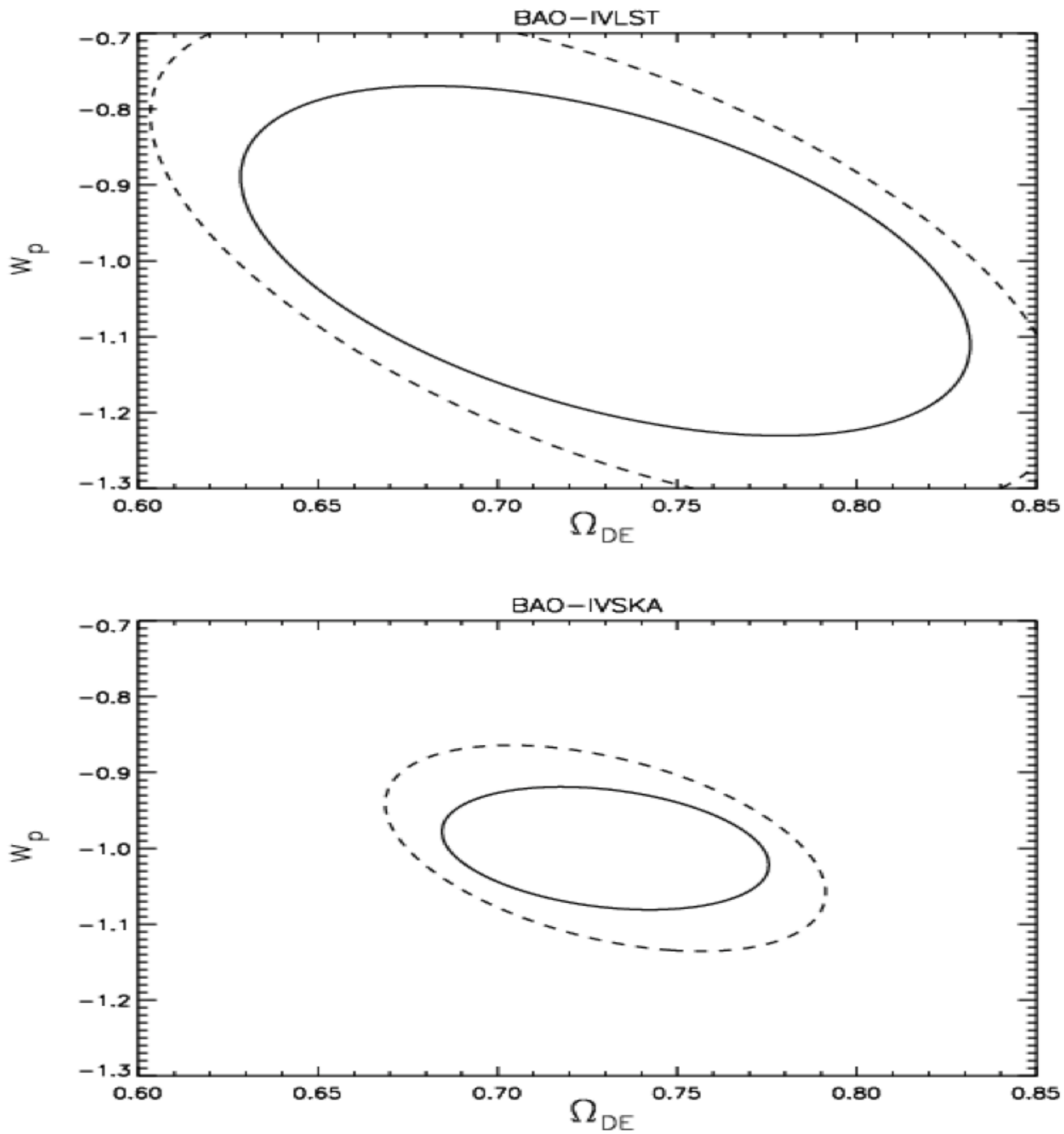

DETF

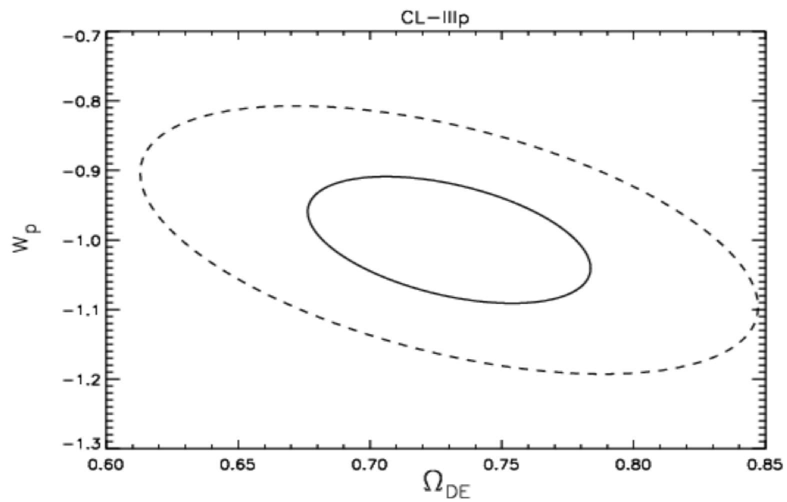

Dashed contours represent pessimistic projections and solid contours represent optimistic projections.

MODEL	$\sigma(w_0)$	$\sigma(w_a)$	$\sigma(\Omega_{DE})$	a_p	$\sigma(w_p)$	$[\sigma(w_a)\times\sigma(w_p)]^{-1}$
CL-IIIp-o	0.256	0.774	0.022	0.672	0.037	35.21
CL-IIIp-p	0.698	2.106	0.047	0.670	0.078	6.11

Data models are denoted by
TECHNIQUE-STAGE+QUALIFIER-OPTIMISTIC/ PESSIMISTIC.

TECHNIQUE	STAGE	QUALIFIER		OPTIMISTIC/PESSIMISTIC	
BAO	I	s	spectroscopic survey	o	optimistic
CL	II	p	photometric survey	p	pessimistic
SN	III	LST	Large Survey Telescope		
WL	IV	SKA	Square Kilometer Array		
		S	Space		

For each data model we present the assumptions regarding statistical and systematic uncertainties. While the statistical performance is reasonably straightforward, the key is systematic errors. Considerable effort and thought went into our projections. It is absolutely crucial that any proposed project justify its systematic error budget.